# IPACK2018-8422

# IMPACT OF INTERNAL DESIGN ON THE EFFICIENCY OF IT EQUIPMENT IN A HOT AISLE CONTAINMENT SYSTEM - AN EXPERIMENTAL STUDY

# Sadegh Khalili

State University of New York at Binghamton-SUNY Binghamton, NY, USA

# **Husam Alissa**

Microsoft Redmond, WA, USA

# Kourosh Nemati,

Future Facilities Inc. San Jose, CA, USA

# **Mark Seymour**

Future Facilities Ltd. London, UK

# **Robert Curtis, David Moss**

Dell Austin, TX, USA

# **Bahgat Sammakia**

State University of New York at Binghamton-SUNY Binghamton, NY, USA

#### **ABSTRACT**

There are various designs for segregating hot and cold air in data centers such as cold aisle containment (CAC), hot aisle containment (HAC), and chimney exhaust rack. These containment systems have different characteristics and impose various conditions on the information technology equipment (ITE). One common issue in HAC systems is the pressure buildup inside the HAC (known as backpressure). Backpressure also can be present in CAC systems in case of airflow imbalances. Hot air recirculation, limited cooling airflow rate in servers, and reversed flow through ITE with weaker fan systems (e.g. network switches) are some known consequences of backpressure. Currently there is a lack of experimental data on the interdependency between overall performance of ITE and its internal design when a backpressure is imposed on ITE. In this paper, three commercial 2-rack unit (RU) servers with different internal designs from various generations and performance levels are tested and analyzed under various environmental conditions. Smoke tests and thermal imaging are implemented to study the airflow patterns inside the tested equipment. In addition, the impact leak of hot air into ITE on the fan speed and the power consumption of ITE is studied. Furthermore, the cause of the discrepancy between measured inlet temperatures by internal intelligent platform management interface (IPMI) and external sensors is investigated. It is found that arrangement of fans, segregation of space upstream and downstream of fans, leakage paths, location of sensors of baseboard management controller (BMC) and presence of backpressure can have a significant impact on ITE power and cooling efficiency.

#### NOMENCLATURE

**BMC** baseboard management controller

cold aisle containment
central processing unit
hot aisle / cold aisle
hot aisle containment
hybrid containment
inlet air temperature, °F (°C)

IPMI intelligent platform management interface

information technology IT

ITE information technology equipment

Р pressure, in. wc (Pa) PUE power usage effectiveness

RU Rack Unit

SAT supplied air temperature, °F (°C)

temperature, °F (°C) thermal design power TDP

leakage ratio X

# INTRODUCTION

In today's world, almost every aspect of modern life, including healthcare, communications, airlines, government, business, entertainment, security, education, and more depend on electronics and information technology - the key components of data centers. Data centers are mission-critical facilities responsible for storing, processing, handling and managing huge amounts of information data, and have been growing fast to propel the expanding demand for information technology (IT) services. Energy efficiency has become the most common concern in the data center industry due to the fast growth of power consumption and increasing concern about the impact of the related carbon emissions on the environment. A recent study by Shehabi et al. [1] estimates 73 billion kWh power is projected to be consumed in U.S. data centers in 2020 that is equivalent to

the amount consumed by about 6.8 million average American homes in 2015. This is when the cooling system consumes about a third to half of the total power consumption in a data center [2]. Therefore, a few percentage increase in the cooling efficiency can lead to considerable energy savings. In addition to energy efficiency, reliability is another important factor in data centers. The absolute continuity of services is vital for health-care, telecommunications companies, and banks. In a recent cost analysis of data center outages by Ponemon and Vertiv [3], the downtime impact of unplanned outages was estimated to be up to \$17,200 per minute loss (\$8,851 per minute on average). In this report, ITE failure is found to cause the highest outage cost between all the primary root causes of the outages. This demonstrates the importance of reliability of ITE in data centers.

The cooling infrastructure of data centers is often controlled based on room environmental conditions. One of the most important parameters in this matter is the air temperature at the inlet of servers. Two common methods for monitoring inlet air temperature (IAT) are utilizing data from a network of discrete sensors, and available data from IPMI. The quality and relevance of the collected data can have a significant impact on the reliability and overall efficiency of cooling in data centers. Tradat et al. [4] studied the impact of data collection methods, namely discrete and IPMI data, on the cooling management in a data center. They observed a large variation between IPMI IAT data from ITE in different locations of a neutrally provisioned CAC system, while discrete sensors showed a more homogeneous temperature field inside the CAC. In addition, their results showed that the difference between IPMI and discrete sensors is higher in an under-provisioned CAC system.

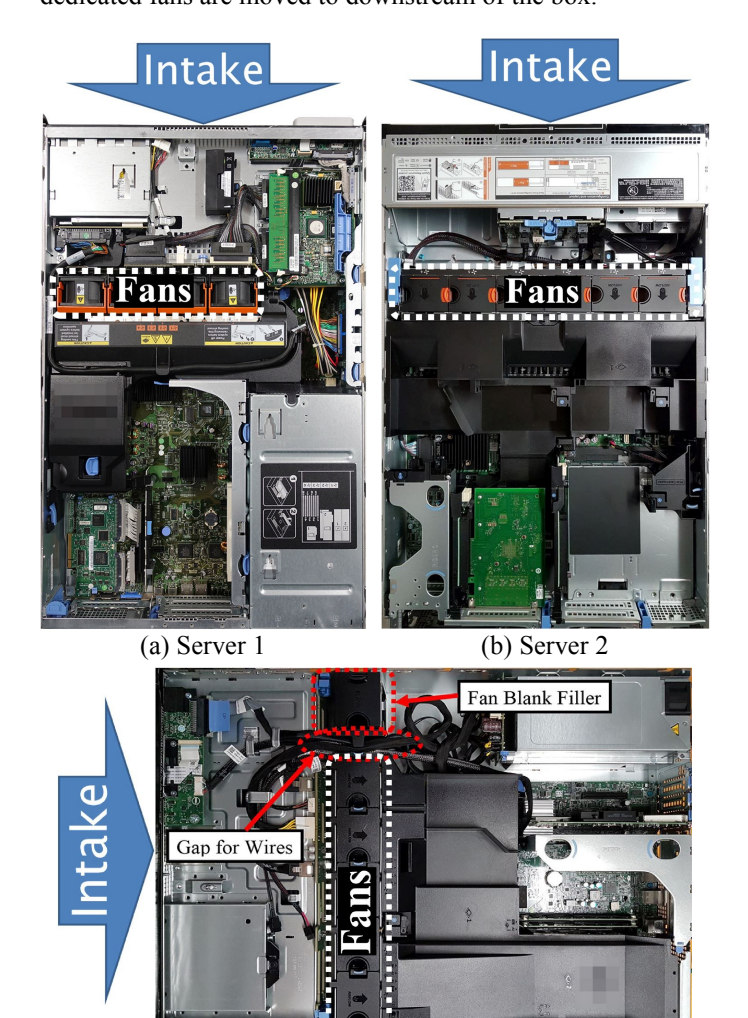
In a legacy air-cooled data center, the server racks are arranged in a standard hot aisle/cold aisle (HA/CA) arrangement and cooling units supply cool air to the cold aisles through a raised floor. The fans of ITE are responsible for drawing cold air from the room to cool their internal components. After cooling server components, air exits the server with an elevated temperature and is returned to cooling units and recirculated. More efficient cooling can be achieved by segregating hot and cold aisles (containment). Containment systems can be divided into CAC, HAC, and hybrid containment (HC). The cold and hot spaces are enclosed in CAC and HAC systems, respectively. In an HC system, both the hot and cold aisles are contained which allows isolated high-density racks, and different work environment conditions in a data center. In CAC systems, cold air is enclosed within the cold aisle and the hot air exhaust from ITE is returned to cooling units through the rest of room space. Sundaralingam et. al [5] experimentally characterized standard HA/CA, partial CAC, and fully contained CAC systems. The benefits of sealing a CAC system using grommets and blanking panels is investigated by Makwana et al. [6]. Khalili et. al [7] studied the impact of tile design on the thermal performance of open and enclosed aisles. On the other hand, HAC segregates hot air within the containment and routes it back to the cooling units' return vent by a drop ceiling or a chimney. Nemati et. al [8] compared steady-state and transient thermal behavior in CAC, HAC and chimney systems numerically. Recently, Khalili et al.

[9] analyzed passive and active HAC and HC systems experimentally. Both CAC and HAC systems can present significant energy saving opportunities in legacy data centers. While all the containment strategies aim to minimize the mixing of hot and cold air, they have different characteristics that can lead to different work environment conditions, power usage effectiveness (PUE), and economizer mode hours [10]. In addition, the behavior of data centers with different containment systems varies significantly in case of airflow imbalances such as a sudden change in IT load or airside cooling failure. Alissa et al. [11] performed an experimental study on airside cooling failure in a CAC system. They noticed a significant difference between available uptime based on the external IAT measurements, and the intelligent platform management interface (IPMI) data. In other words, compared to the standard hot aisle/cold aisle arrangement, their results showed a longer available uptime in a CAC when external sensors data are considered while IPMI data indicated a shorter available uptime. In fact, the difference in the measured uptime originated from the difference between IAT measured via internal (IPMI) and external sensors. A common issue in HAC systems is the imposed backpressure on ITE. Khalili et al. [9] showed that presence of backpressure in HAC and HC systems can lead to an elevated fan speed of ITE, and also cause a discrepancy between IAT measured by internal (IPMI) and external (discrete) sensors  $(\Delta T_s)$ . Also, they observed that presence of backpressure can increase the power consumption of a rack by up to 25%. The fans' speed in a server is regulated to maintain component temperatures in a safe range. The BMC is responsible for monitoring the physical state of ITE using built-in sensors, and adjusting fan speed based on various parameters such as central processing unit (CPU) utilization, IAT, components temperature, etc. An elevated fan speed naturally translates to higher power and operating costs. In addition, a higher fan speed leads to a higher noise level, shorter expected fan lifetime and consequently, a lower overall reliability of the server. Therefore, it is perceived that presence of backpressure can be influential on the efficiency, reliability and thermal performance of ITE.

In the past decades, the increasing power density of ITE has urged engineers to optimize the servers' thermal design. In addition, the growing tendency for utilizing free cooling as well as decreasing CPU temperatures for improving the reliability and power leakage introduces more challenges to the thermal design of high-performance servers. The aim of this study is to investigate interdependency between the thermal performance of ITE and its internal design. Also, the observed discrepancy between IPMI and discrete sensors data in [4,9,11] urges a server level investigation. For this study, the servers are chosen from different generations and models to represent a wide variety of available commercial servers. In addition, the cause of the discrepancy between the data from IPMI inlet temperature sensor and the discrete sensor is investigated.

## ITE AND EXPERIMENTAL SETUP

In this study, three servers from various generations and performance levels are tested. Figure 1 shows the internal design and arrangement of fans in the servers. Server 1 utilizes two CPUs (each CPU has 4 cores). This server has four fans that span about three-quarters of the server width and are installed upstream of CPU heatsinks. This server utilizes two power supplies as the primary and redundant power supplies. A dedicated fan is located upstream of each power supply unit. Server 2 has a modern internal design and incorporates six fans that span across the entire chassis width. Two CPUs are utilized in server 2 that provide 48 cores. Server 3 incorporates five fans while a wire gap and one fan blank filler occupy the rest of server's width. The wire gap provides space for passing wires from downstream to upstream of fans (Fig. 1c). This server utilizes two CPUs with a total of 40 cores. Table 1 presents the thermal design power (TDP), the base and turbo frequencies and the warning threshold for the CPUs of tested servers. Two power supplies are installed in both servers 2 and 3 while their dedicated fans are moved to downstream of the box.



(c) Server 3
Fig. 1 Internal view of servers with the top cover removed

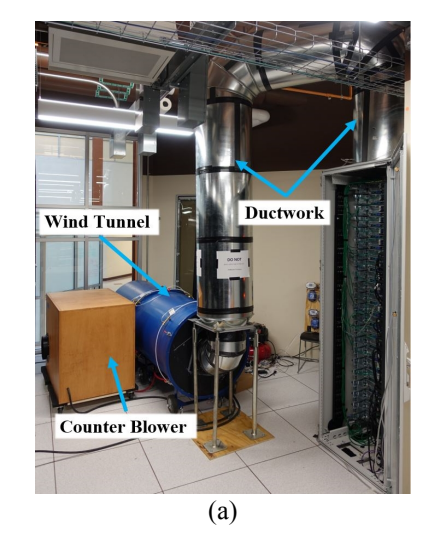
A wind tunnel (in accordance with AMCA 210-99/ASHRAE 51-1999) is utilized for extracting the active flow curves (AFCs) of the servers. Also, the wind tunnel is used to

create various differential pressures across the servers during smoke tests. The airflow through wind tunnel can be calculated by measuring the pressure drop across a nozzle array in the middle of the wind tunnel. The wind tunnel is connected to a blower/counter-blower that can either suck or blow air. The flow rate through the wind tunnel can be adjusted via a solid-state fan speed controller as well as a sliding blast gate at the end of the wind tunnel. Also, the differential pressure between the room and inside the chamber can be controlled by adjusting the supplied flow rate to the wind tunnel. The flow visualization is carried out using a fog generator to investigate the flow field inside, and in the close proximity of the perforations on the servers' chassis.

In addition to bench tests, the servers are tested in a 72-RU chimney rack with an overall dimension of 28" × 48" × 87.5"  $(71 \text{cm} \times 122 \text{ cm} \times 222 \text{ cm})$  to analyze the thermal performance of them when they are stacked in a server rack. A 15" (38 cm) deep chamber is available between the rear door of the rack and servers' outlet. The servers' exhaust air is extracted through an 18" diameter round chimney at the top near the back of the cabinet. The chimney is ducted to the inlet of the wind tunnel (Fig. 2a). This allows controlling the airflow rate and pressure at the outlet of the cabinet (base of the chimney) by regulating the speed of the counter blower. The cabinet is populated with 22 servers and one Cisco Nexus 2248TP-GE Fabric Extender. In this paper, the middle area of the cabinet is selected for deploying servers 2 and 3 while the rest of rack is populated by twenty of servers of type 1 (see Fig. 2c and 2d). The temperature at various locations is monitored using T-type thermocouples as well as Degree-C UAS1200LP airflow and temperature sensors (Fig. 2d). The differential pressure between the room and the hot aisle is measured at the bottom, middle and top of the HAC. The locations of pressure probes are outlined in blue in Fig. 2b.

Table 1: Processor information for servers in this study

Ser.	Processor	TDP	Base Freq.	Turbo Freq.	Warning
#	(Intel Xeon)	(W)	(GHz)	(GHz)	threshold
1	E5345	80	2.33	N/A	192.2°F (89°C)
2	E5-2687WV4	160	3.00	3.50	197.6°F (92°C)
3	E5-2630V4	85	2.20	3.10	185°F (85°C)





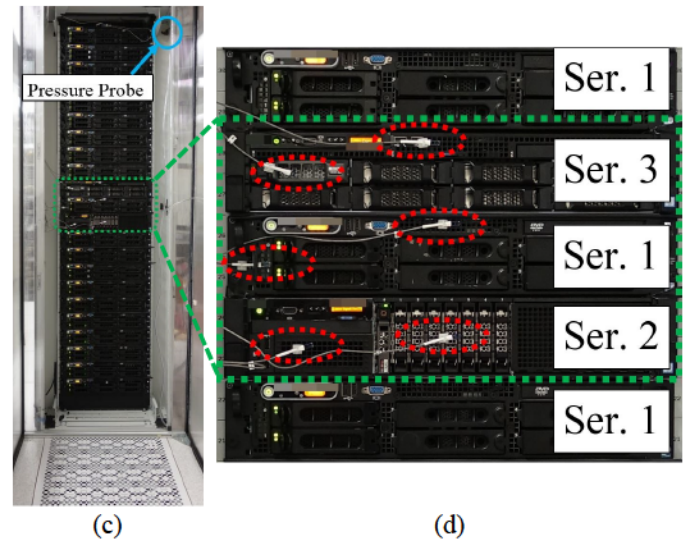


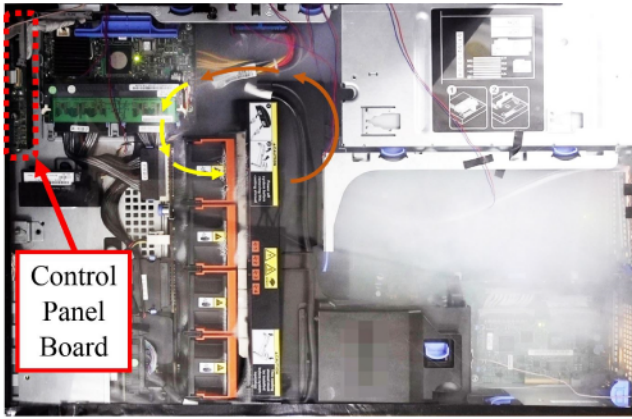
Fig. 2: Chimney exhaust cabinet, wind tunnel, and instrumentations: a) chimney ductwork and wind tunnel, b) location of pressure probes in HAC with the rear door open, c) location of servers in the middle of the cabinet, d) location of discrete temperature sensors in the CA.

#### STUDY CASES

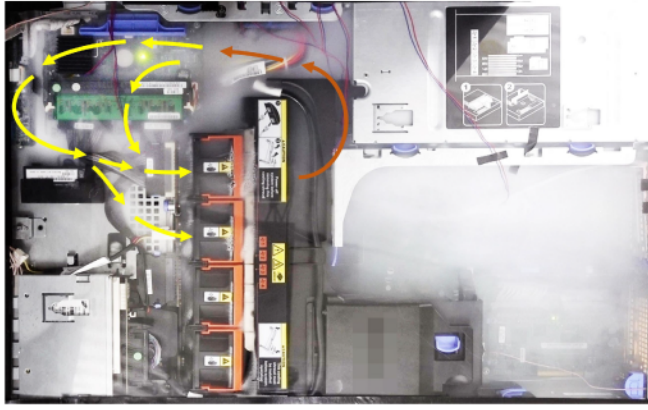
#### **Internal Recirculation in server 1**

The goal of server thermal design is to dissipate the generated heat and maintain the components temperature in a safe range with a minimal expenditure of energy and component cost. The BMC in a server is responsible for measuring internal physical variables such as temperature, fan speeds, power supply voltage, operating system functions, etc. In most servers, an internal temperature sensor is implanted in the control-panel board in front of the server to monitor IAT. A discrepancy between the built-in IPMI sensor and external IAT sensor in front of server 1 has been observed in multiple studies [9,11,12]. A consistent phenomenon can be observed in these studies, which is a relationship between  $\Delta T_s$  and backpressure. However, the cause of this phenomenon has not been investigated.

The internal design of server 1 is shown in Fig. 1a. This server utilizes four fans for cooling the CPU and main components, and one dedicated fan upstream of each power supply unit. In server 1, server fans span about three-quarters of the server's width. Installing the server fans in only a portion of the server width leaves a gap which allows for internal recirculation due to the pressure differential between upstream and downstream of the fans. An internal recirculation has been known as a phenomenon that decreases the cooling performance in ITE. In this phenomenon, a portion of air, after entering the ITE and cooling hot components, does not leave the chassis and recirculates inside the ITE. Therefore, hot air mixes with the fresh cold air from intake which increases the coolant temperature. This mix of hot and cold air streams has some known consequences, such as reduced cooling capacity, hot spot occurrence, and decreased thermodynamic efficiency. Figure 3a to 3c shows that the extent of the area affected by recirculation expands with back pressure. This means that if the backpressure is high enough, the recirculation can reach the control-panel board where the IPMI IAT sensor is located. In this case, the recirculation can affect the readings of IPMI IAT sensor. As a discrete sensor in front of the ITE may not see this recirculation, it can cause a discrepancy between readings of IPMI IAT and external sensors ( $\Delta T_{\rm s}$ ). Hence, in servers with a similar internal design to server 1, the magnitude of  $\Delta T_{\rm s}$  can depend on the magnitude of backpressure.



(a) Free delivery point (no backpressure)



(b) Backpressure = 0.04 in wc (10 Pa)



(c) Backpressure = 0.1 in wc (25 Pa)

Fig. 3: Smoke tests demonstrate the impact of backpressure on the extent of internal recirculation

The variation of IPMI and discrete IATs with backpressure in server 1 is presented in Fig. 4. In this experiment, the server is tested in an isothermal environment which means air temperature at both the intake and surroundings of the server are controlled at 68 °F (20 °C). In a typical rack with blanking panels installed, the space in front of the server is separated from a hot zone behind the rack's front face. A hot air leakage from hot zone into server chassis (e.g. from perforations on the chassis, or through a disconnected or removed power supply) can also affect the internal temperature and flow fields, which may enhance the  $\Delta T_{\rm s}$ . Hence, server 1 is tested in an isothermal environment to focus on the impact of backpressure as an isolated parameter and eliminate potential impacts of temperature in the hot zone  $(T_{hz})$ . Figure 4 shows that  $\Delta T_s$  is minimal when a negative backpressure is imposed on the server. However, at free delivery point (zero backpressure),  $\Delta T_s$  begins to increase. This discrepancy increases to 9°F (5°C) when backpressure is 0.1 in. wc (25 Pa). In addition, a slight increase in the discrete IAT is seen in backpressures higher than 0.05 in. wc (12.5 Pa). This is due to expansion of recirculation to outside of chassis, i.e. hot air leakage from inside the chassis to the space in front of the server. This leakage is shown in Fig. 5. In addition, it is observed that fan speed starts to increase when IPMI IAT reaches to 78 °F (26 ° C) which is the threshold for server 1. Furthermore, Fig. 4 shows that the difference between CPUs' temperature increases with back-pressure. In server 1, CPU B is exposed to the internal recirculation and experience higher temperatures. It is worth repeating that that the data in Fig. 4 are extracted when supply air temperature (SAT) was 68 °F (20 °C) in an isothermal environment. Therefore, server fans may ramp up at a lower backpressure when SAT is higher or if hot air can leak into the chassis.

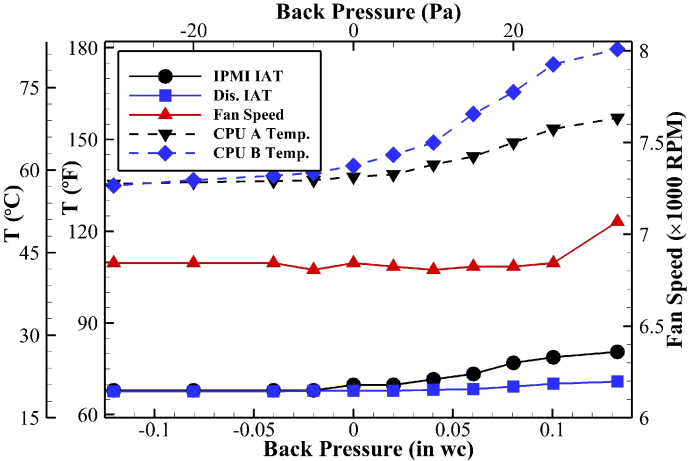


Fig. 4: Variation of IPMI IAT, discrete IAT, CPU temperatures and averaged fan speed with backpressure



Fig. 5: Internal recirculation can expand to CA

To eliminate this internal recirculation, server fans can be spanned across all width of a server, be moved to the rear of the server or rack level fans can be utilized instead of dedicated server fans. However, this would create a negative pressure inside chassis (upstream the fans) that may enhance the leakage from hot zone through chassis openings. This potential problem can be addressed by installing side panels on the cabinets' mounting rails to segregate the servers' zone from the hot zone.

#### Perforations on the Chassis of Server 2

In a typical server, system fans draw in cold air through front panel to cool the internal components such as hard disk drives (HDDs), CPUs, memory modules, etc. Therefore, in a typical server rack, the front panel of a server is in contact with the supplied cold air while the rest of chassis is exposed to air with an elevated temperature in the hot zone. In the CAC systems, the maximum SAT is limited to obtain an acceptable environment for non-racked ITE and bearable work temperature for staff while this limit does not apply to HAC systems which allow a higher SAT. As a result, the air temperature inside the hot zone can be significantly higher than an analogous CAC although HAC generates a cooler environment in the data center room as a whole. In addition, each containment system has different airflow paths and leakage characteristics. Hence, environmental conditions in which the chassis is placed (inside of cabinets) can be significantly different between HAC and CAC systems.

In most ITE, openings with different geometry and size can be found on the sides of a chassis for various purposes such as improving access to fresh air (by increasing air intake area), balancing the internal pressure field, weight reduction as well as mounting needs. However, if these perforations are located upstream of server fans, they can provide a path for recirculation from hot zone through the server which can have a negative impact on the efficiency and performance of server's cooling system. In addition, this recirculation can cause local hot spots inside a server. Figure 6 shows the airflow visualization near the top perforations for server 2 operating at its free delivery point (no backpressure). The top cover is replaced by an acrylic sheet for this test. The smoke visualization demonstrates air entry through the openings on top near the front of this server that is due to the low-pressure field upstream the server fans. An interesting observation is that this leakage can significantly affect readings of IPMI IAT sensor. The IPMI IAT sensor is usually located in front of the chassis to monitor air temperature at the intake of a server. In server 2, this sensor is mounted on the control-panel board which is located under the perforated area on top near the front of the chassis. The location of IPMI IAT sensor is outlined in red on the pushed-out control panel in Fig. 6. Consequently, air leakage from hot zone through top perforations can pass over the IPMI IAT sensor and affects its measurements. To study the impact of hot zone temperature on the IPMI IAT, hot air at various temperatures is supplied to a local chamber on the top of server 2 (see Fig. 7). Presence of chamber allows simulation of a hot zone with various temperatures without affecting air temperature at the intake of server when no backpressure is imposed on the server. The air

temperature inside the chamber  $(T_{hz})$  is varied from 68 °F (20 °C) to 104°F (40°C) during the test while SAT is maintained at 68°F (20°C). A temperature sensor is placed on top of the perforated area to monitor and record the air temperature through the perforated area. Figure 8 presents the variation of IPMI IAT data. average of fans speed as well as temperature and utilization of CPUs in server 2 with  $T_{\rm hz}$ . It is observed that IPMI IAT increases with  $T_{\rm hz}$  proportionally. The average difference between IPMI IAT and  $T_{\rm hz}$  for the presented data points is measured less than 1  $^{\circ}$ F (0.5 °C) which is less than the claimed accuracy for the IPMI IAT sensor [13]. Therefore, the  $\Delta T_s$  is not due to low accuracy of IPMI sensors in server 2 but is due to hot air leakage through top perforations. In addition, this observation demonstrates the potential impact of chassis design and location of IPMI sensors on the thermal performance of a server. In addition, a surge increase in fans speed is seen when IPIM IAT exceeds the ASHRAE IAT limit (35°C) for class A2 ITE. In addition to higher power consumption due to elevated fan speed, this surge increase can affect the pressure field inside contained spaces and lead to a potential instability in cooling systems of a data center.



Fig. 6: Air enters the chassis through perforations on the top of server 2

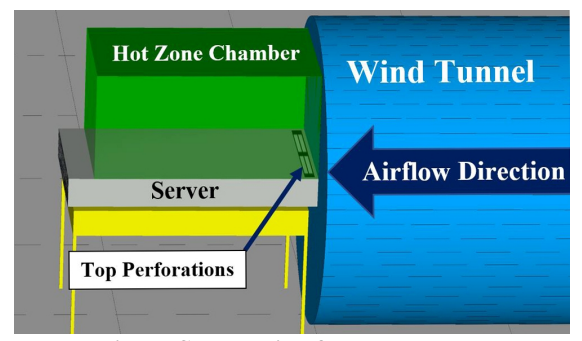


Fig. 7: Schematic of the test bench

In this test, CPUs are exercised fully with executing an input/output command repeatedly when tasks are pinned to CPU cores. The processor utilizations above 100% is due to CPU frequency scaling because the CPU frequency governor is set to performance mode. Interestingly, a slight CPU throttling is observed when IPMI IAT reaches to 99°F (37°C) while CPU temperature is significantly lower than the earlier data points (which is because of higher airflow rate due to elevated fan

speed). It is perceived that CPU throttling in this test is a safety action by BMC as an open loop response to IPMI IAT. It is observed that the magnitude of utilization drop due to this open loop action depends on the CPU stressing application (core bound versus input/output bound benchmarks). For example, a 25% drop in CPU utilizations was observed under the same conditions when CPUs were stressed using MPrime [14]. However, the throttling seems unnecessary as the CPU temperatures are much lower than the warning threshold of the CPUs (see Table 1). Therefore, it is seen that a false high IPMI IAT can reduce the computational performance of a server depending on the implemented safety strategies.

Figure 9 shows the path of airflow inside server 2 when smoke is introduced from the front intake. It is observed that air travels through the chassis from front intake to the rear side of the server with minimum internal recirculation. This is achieved by distributing the fans across the chassis width as well as a good segregation of the space downstream of the server's fans from the upstream space.

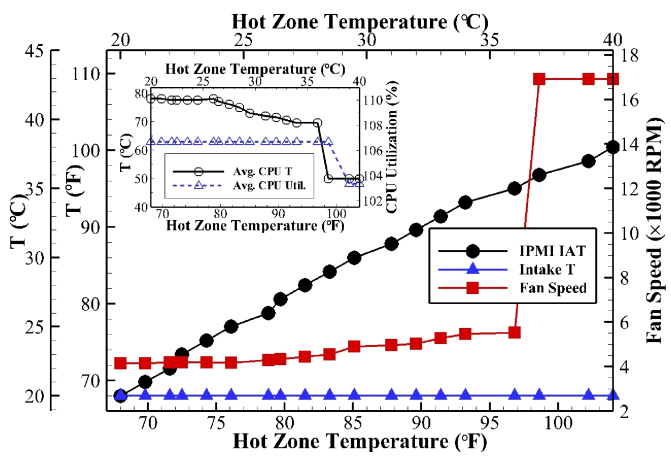


Fig. 8: Impact of  $T_{hz}$  on the performance of server 2

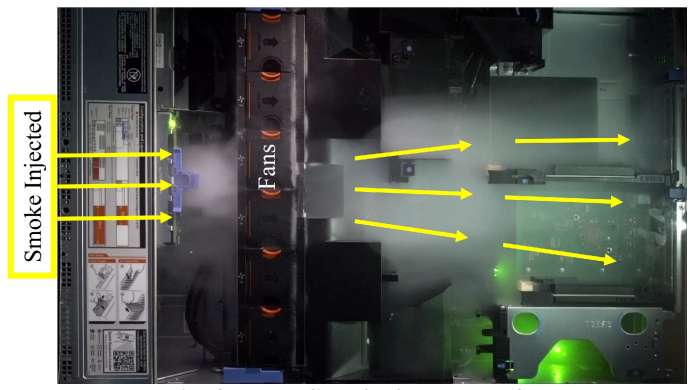


Fig. 9: Flow field inside server 2

Figure 10 presents the relation between airflow rate and backpressure (AFC) for server 2 with fans set to operate in the high-speed mode (approximately 13,800 RPM). The server is mounted on the wind tunnel and AFC is extracted by measuring the differential pressure between inside the wind tunnel's chamber and room for various flow rates. The fan affinity laws

can be utilized for estimating the ITE flow for lower fans' RPM [15]. In AFC tests, it is assumed that impact of a negative pressure inside the chamber is identical with when a positive backpressure of the same magnitude is imposed on the server.

Two cases are compared in Fig. 10. In the first case, the top perforations are left open (typical condition) while the perforations are sealed in case 2. The difference between flow rates of the two cases at each backpressure can be assumed to be equal to the airflow rate though top perforations (leakage rate) in case 1, i.e. the leakage rate is calculated by deducting flow rate at the front intake of the server in case 1 from the flow rate in case 2. The leakage ratio x can be defined as the ratio of the rate of leakage to the total airflow through the server (which is equal to intake flow rate in case 2).

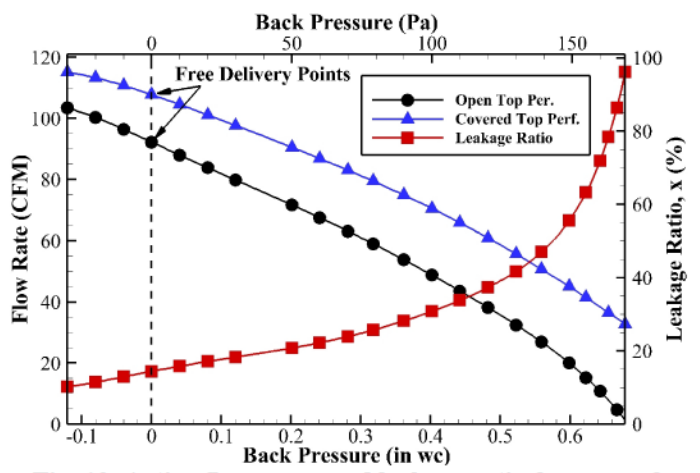


Fig. 10: Active flow curve and leakage ratio for server 2

$$x = \text{Leakage ratio} = \frac{FR_{\text{covered top perforations}}^{\text{intake}} - FR_{\text{open top perforations}}^{\text{intake}}}{FR_{\text{covered top perforations}}^{\text{intake}}}$$
(1)

Figure 10 shows that at the free delivery point the leakage ratio is about 15% of the total airflow rate. It can be proved that x is independent of the server fan speed by implementing affinity laws. This leakage can mix with cold air from front intake and raise the cooling air temperature. The temperature of mixed streams ( $T_{\rm mix}$ ) can be calculated by implementing the energy equation for mixing of two fluid streams combined with conservation of mass. By neglecting heat transfer to and from the chassis, changes in air properties, potential energy, kinetic energy, and work as well as assuming that the two streams mix into a homogenous fluid,  $T_{\rm mix}$  can be written as:

$$T_{\text{mix}} = (1 - x) T_{\text{in}} + x T_{\text{hz}}$$
 (2)

where  $T_{\rm in}$  and  $T_{\rm hz}$  are intake and hot zone air temperatures, respectively. Therefore, the temperature rise due to the leakage through top perforations for this server can be written as:

$$\Delta T_{\text{coolant}} = T_{\text{mix}} - T_{\text{in}} = x \left( T_{\text{hz}} - T_{\text{in}} \right) \tag{3}$$

By implementing Eq. (3), a quick calculation reveals that for a 20 °C difference between  $T_{\rm hz}$  and  $T_{\rm in}$ , at the free delivery point (where x=0.15),  $\Delta T_{\rm coolant}$  is 3 °C. Hence, a data center operator may choose to decrease the SAT to compensate for this temperature rise. It is worth mentioning that only one hard disk

drive (HDD) was installed on the front panel of server 2 (maximum capacity is 16 HDDs) during the tests. Therefore, significantly higher leakage ratios (x) can be anticipated when the entire front of chassis is populated by storage drives due to increased airflow impedance at the front intake. This in turn, can lead to higher  $\Delta T_{\rm coolant}$ . On the other hand, these perforations can help the server to capture more fresh air in presence of a negative backpressure (in an over-provisioned containment) or if a gasket is placed behind the top perforations. A proper gasket allows access to fresh air from the cold aisle and eliminate hot air recirculation from the hot zone. It should be noted that installing narrow gaskets in the gap between front panel of servers can block the access to cold air entirely and worsen the situation.

# Combined Impact of Top Perforations and Internal Recirculation – Server 3

In this section, the airflow design in server 3 is analyzed. One row of perforations is designed on the top cover of server 3 (compared to two rows on the chassis of server 2). One out of eight available drive bays is filled with a 3.5 in. HDD while the remainder of bays is blanked using standard HDD blank fillers. It should be mentioned the HDD blank fillers do not blank the bays completely and allow some airflow. Server 3 utilizes five server fans and a fan blank filler as shown in Fig. 1c. In addition, a gap is designed between the fan array and the fan blank filler for passing the wires from mainboard (downstream of fans) to the control-panel board and to the hard drive backplane board. Presence of the fan blank filler can decrease the internal recirculation significantly (compare to server 1 which does not utilize any fan blank filler). However, the installed blank filler allows some leakage due to its design and orientation of installation. In addition, the wire gap provides a path for internal recirculations. Figure 11 demonstrates the presence of recirculation in server 3. Similar to server 1, the extent area affected by the recirculation depends on the magnitude of backpressure imposed on server 3. Smoke tests carried out for various magnitudes of backpressure from 0 in wc to 0.1 in wc (25 Pa). The results showed that recirculation does not reach the control-panel board. Therefore, it is expected that backpressures bellow 0.1 in wc (25 Pa) have minimal impact on the IPMI IAT sensor for the current server configuration.

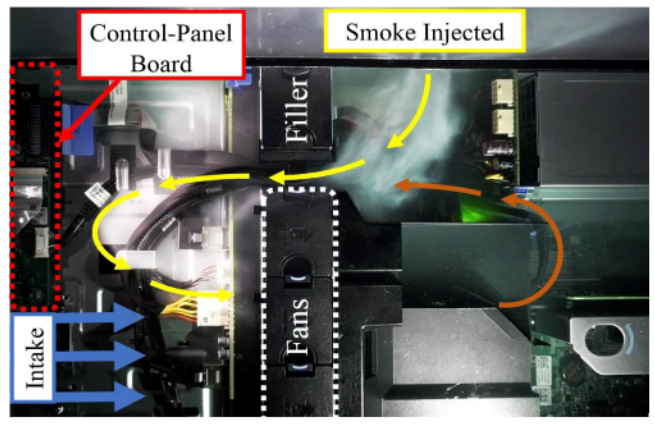


Fig. 11: Internal recirculation in server 3

To study the impact of the presence of top perforations on the performance of server 3, this server is tested under a similar test procedure for server 2. Figure 12 shows that IPMI IAT changes with air temperature in the hot zone which proves the impact of  $T_{\rm hz}$  on the IPMI IAT sensor. In addition, a continuous increase in average fans speed with IPMI IAT is seen. It should be mentioned that the fans speed reached to 17,000 RPM at IPMI IAT of 122°F (50°C) which is not included in Fig. 12. Also, no significant increase in the CPUs temperature is seen during the test. This indicates that the change in fan speed was mainly due to variation of IPMI IAT. Furthermore, opposite to server 2, no CPU throttling due to high IPMI IAT (up to 122°F (50°C)) is observed in server 3. By comparing Figs. 8 and 12, it is seen that the fan speed response to IPMI IAT in servers 2 and 3 is significantly different although these servers are from the same manufacturer and generation. Figure 13 presents the extracted AFCs for server 3. Four cases are investigated for gaining a better understanding of the impact of internal recirculation and chassis' perforations on the airflow field inside the server. The first case represents the original factory shipped condition of the server. In the second case, the wire gap and fan blank filler are sealed. The top perforations are sealed in the third case. Finally, in the fourth case, the combination of second and third cases is considered in which the wire gap, fan blank filler, and top perforations are all sealed.

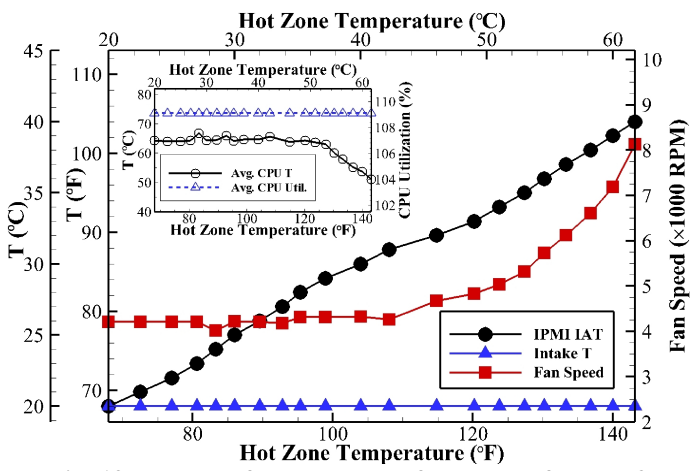


Fig. 12: Impact of  $T_{hz}$  on the performance of server 3

To quantify the impact of internal recirculation and leakage through the top perforations on the air draw from cold aisle, the area in front of blank filler and wire gap is sealed using foam gasket. Also, foam tape is used to seal the space between fans and the server's top cover. It is observed that the air draw through front panel (cold aisle) increases by sealing the internal gaps and top perforations. Figure 14 shows that this increase is about 11% at the free delivery point of the server with respect to the original condition of the server. Also, it is found that sealing the top perforations can increase the airflow rate at the front intake by 13%. Finally, a 25% increase in intake flow rate is observed in the combined case when no backpressure was imposed on server 3. In addition, Fig. 14 shows that the magnitude of flow rate

improvement is higher at higher backpressures. An increase in rate of air draw from the cold aisle would decrease the temperature of the components as well as air at the outlet. As a result, the fan speed can also be reduced which in turn can lower the chiller load and operational costs in a data center.

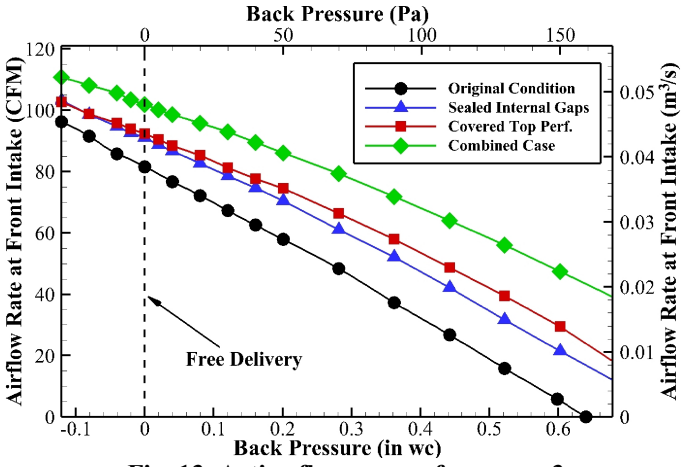


Fig. 13: Active flow curves for server 3

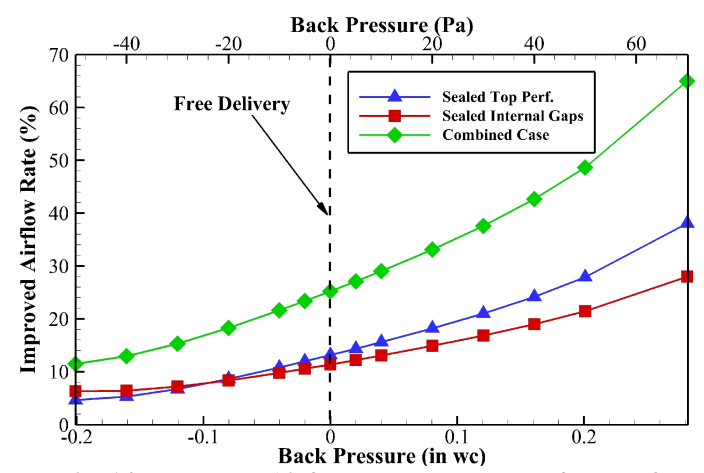


Fig. 14: Improved Airflow at Front Intake of server 3

## Case Study: Testing Servers in a Chimney Exhaust Cabinet

In this section, two scenarios are considered to investigate the impact of backpressure and hot air recirculation through top perforations on thermal performance of the servers. The ITE are tested in a chimney rack that represents a HAC system (see Fig. 2). Nemati et. al [8] showed that pressure at the outlet of a chimney rack can be negative, zero or positive depending on the distance between the cabinet and cooling units. In this study, the pressure at the outlet of the cabinet (base of chimney duct) is controlled at 0 Pa. It should be noted that all the pressure measurements in this section are differential pressures with respect to the room pressure. In this section, SAT is controlled at 73 °F (23 °C) and CPUs are stressed fully at the beginning of the tests. Two scenarios are considered: In the first scenario, the gaps between servers are covered by placing narrow gaskets between front panels of ITE to achieve a good segregation between hot and cold aisles. However, the top perforations of servers 2 and 3

are not covered by sealing strips in this scenario. In other words, the perforations had access to air from hot zone. In the second scenario, a gasket is placed behind the perforated area on the chassis of servers 2 and 3, and the test procedure for scenario 1 is repeated. Finally, the test is repeated with no sealing strips between front panels of servers. After assuring a steady state, at t = 1,250 seconds hot aisle is enclosed by closing the rear door of the cabinet. Figure 15 presents the pressure variation in hot and cold aisles during the test. It is seen that pressure inside HAC experiences a sharp increase to 0.03 in wc (8 Pa) after enclosing hot aisle at t = 1,250s. After the initial abrupt change, a continuous increase in  $P_{\text{HAC}}$  with time is observed until it reaches to 0.104±0.004 in wc (26±1 Pa). This increase is due to rise in servers' fan speed. Figure 16 shows the variation of fan speed during the test period. It is seen that introducing CPU load (at t = 0) slightly increased the fans speed of servers 2 and 3. After enclosing hot aisle, a significant increase in fan speed of servers 1 and 2 is observed while this increase is smaller in server 3. As was shown in Fig. 8, a surge increase in the fans speed of server 2 is expected when IPMI IAT reaches to 36°C. Therefore, the fluctuations in fan speed of server 2 is due to oscillations in IPMI IAT of this server between 35 and 36 °C (see Fig. 17).

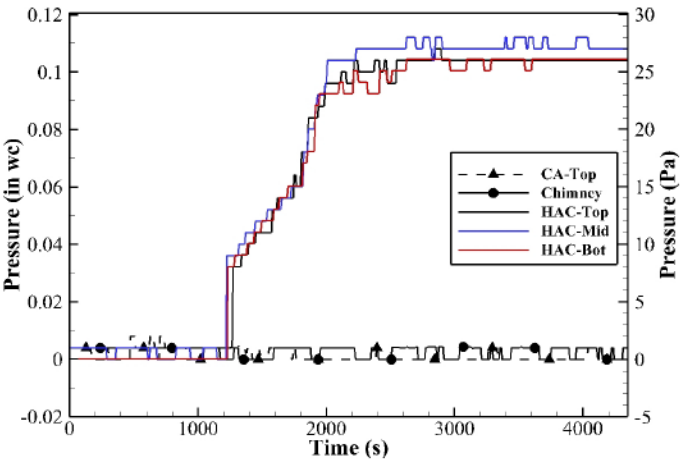


Fig. 15: Pressure inside hot and cold aisles - Scenario 1

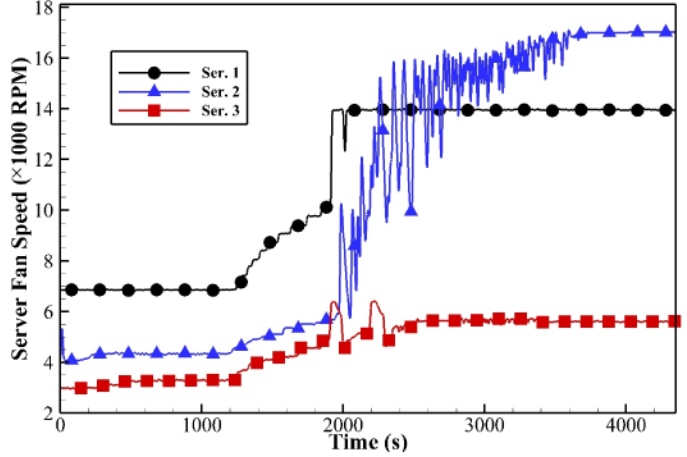


Fig. 16: Variation of averaged fans speed - Scenario 1

The variation of inlet temperature data from IPMI and discrete sensors are presented in Fig. 17. It is seen that IPMI IAT and  $\Delta T_s$  increases with backpressure. Figure 18 presents the variation of CPU temperatures with time. The CPUs experienced an initial increase in their temperature after enclosing hot aisle. This temperature rise is due to the abrupt change in backpressure which limits the servers' airflow rate. However, CPUs' temperature either remains fairly constant or decreases with time as the fans ramp up. Therefore, it is perceived that the continuous increase in the servers' fan speed with time is mainly due to increase in IPMI IAT of servers.

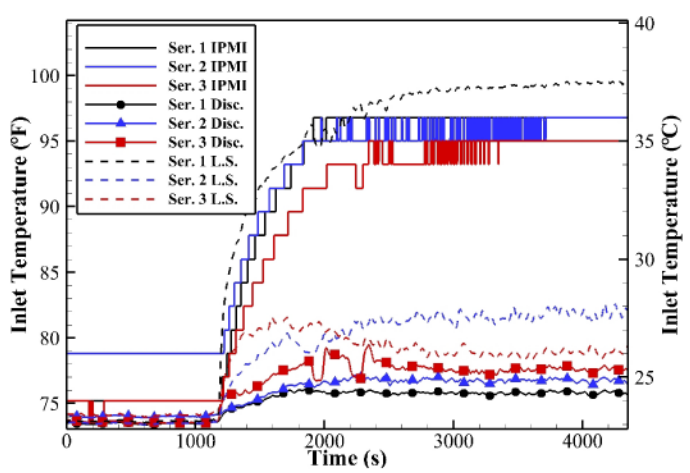


Fig. 17: IAT data for the selected servers – Scenario 1

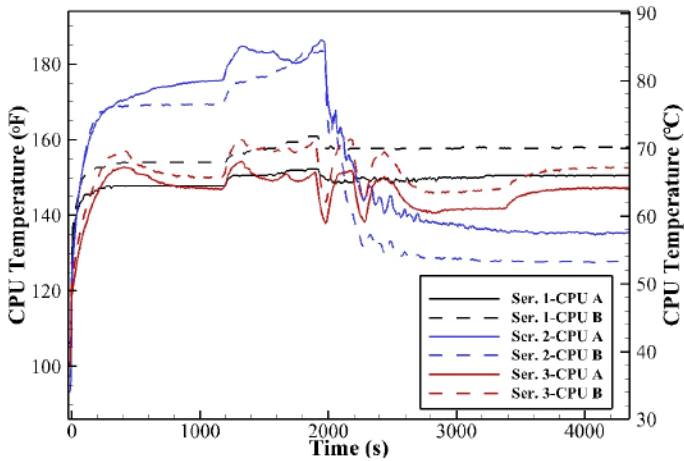


Fig. 18: Temperature of CPU junction of the selected servers – Scenario 1

An interesting observation in Fig. 17 is the high temperature on the left side (L.S.) of servers' intake. Figure 19 presents a thermography of the face of servers at the end of scenario 1 which shows significantly high temperatures on the left side of the servers' front panel. Further investigations reveal a hot air recirculation through the front panel of server 1 (as was shown in Fig. 5). In addition, there are a few openings on the side of chassis of server 1 (see Fig. 20) that allow air leakage from hot zone into cold aisle through the front panel. This leakage along

with the enlarged internal recirculation due to presence of the backpressure affects the readings of the external temperature sensor on the left side of the server as shown in Fig. 17. Furthermore, this leakage from hot zone mixes with supplied airflow to the cold aisle that decreases the cooling efficiency.

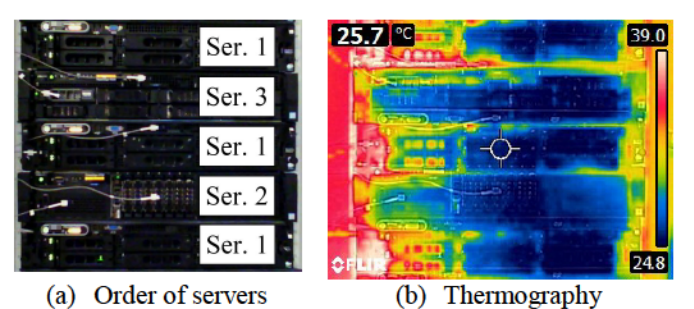


Fig. 19: Thermography from the face of the cabinet at the end of Scenario 1



Fig. 20: Openings on the side of chassis – server 1

In scenario 2, a gasket (built specifically for this experiment) is placed behind the perforated area of servers 2 and 3 as shown in Fig. 21. This gasket allows servers' access to fresh air from cold aisle and eliminates hot air recirculation from hot zone through top perforations. The same test procedure for scenario 1 is repeated for scenario 2. Similar to scenario 1, pressure inside the HAC increases with time. This is because the cabinet is populated with 20 servers of type 1 and only one server of each of types 2 and 3. Therefore, because server 1 is not modified, it is anticipated that servers of type 1 behave similar to scenario 1 (false high IPMI IAT and elevated fan speed) and govern the overall pressure field inside the HAC.

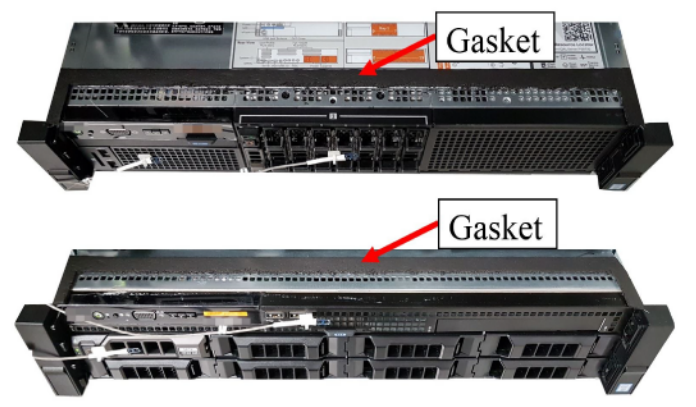


Fig. 21: Location of gaskets for servers 2 and 3 - Scenario 2

From Figs. 22 to 24, it is observed that  $P_{\text{HAC}}$ , fan speed and IPMI IAT of servers 2 and 3 are reduced compared to scenario 1 (Figs. 15 to 17). Table 2 compares the IPMI IAT of the servers at the end of scenarios 1 and 2. Although,  $\Delta T_s$  for servers 2 and 3 in scenario 2 is significantly less than scenario 1, it is still considerable. This can be explained by hot air leakage from servers of type 1 into the cold aisle. As shown in Figs. 2c and d, servers 2 and 3 are surrounded by servers of type 1. Because the top perforations in servers 2 and 3 are the closest intakes to servers of type 1, the leaked hot streams from servers 1 are drawn into servers 2 and 3 through their top perforations, which leads to an elevated IPMI IAT in these servers. Therefore, it can be concluded that leaky servers can affect the performance of their adjacent servers. In addition, ducting top perforations of servers 2 and 3 to cold aisle creates local low pressures near the intake of server 1 which enhances hot air leakage from this server into cold aisle. This in turn increased the IPMI IAT of server 1 from 97°F (36°C) in scenario 1 to 99°F (37°C) in scenario 2.

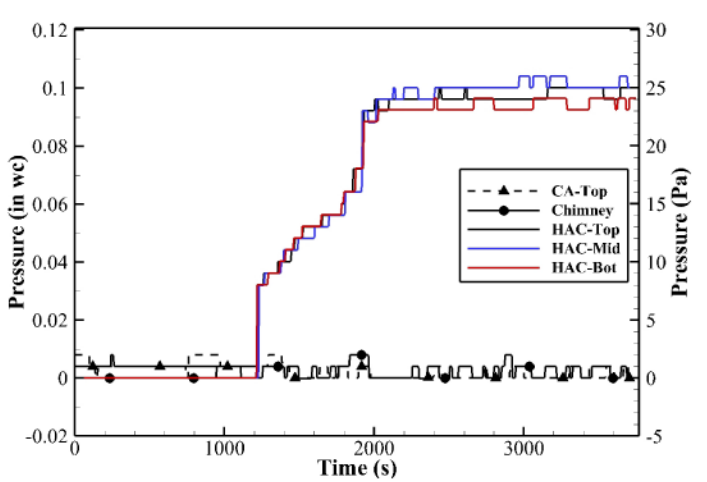


Fig. 22: Pressure inside hot and cold aisles – Scenario 2

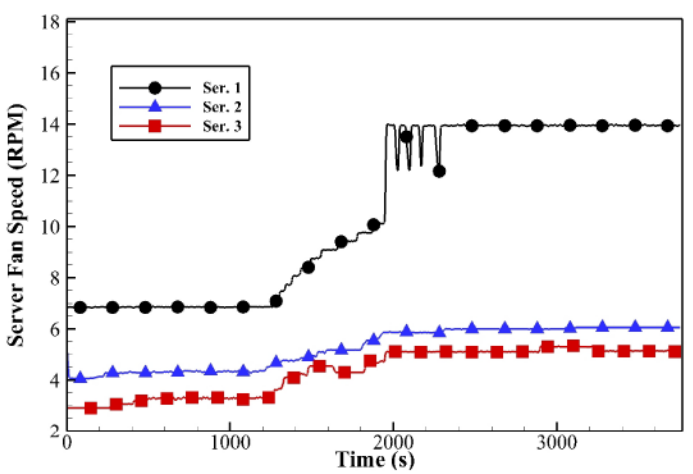


Fig. 23: Variation of averaged fans speed – Scenario 2

Table 2 compares the IPMI IAT, fan speed and percentage of power increase in the selected servers at the end of scenarios 1 and 2. Because no change in CPU utilization was observed

after enclosing the hot aisle, the main cause of increase in the servers' power is the changes in the servers' fan speed. As expected, the power increase for server 1 is equal in scenarios 1 and 2 because this server is unchanged between scenarios 1 and 2. However, power consumption of server 2 is significantly lower at the end of scenario 2 due to the installation of wellpositioned gaskets. Also, a slight improvement is observed in the power consumption of server 3 at the end of scenario 2. The difference between the increase in the power of servers 2 and 3 during the tests is because the fan control strategies in these servers are different from one another (see Figs. 8 and 12). It should be noted that when the CPU utilization in a server is lower, the ratio of the power consumed by fans to the total power consumption of the server is higher (due to lower CPU power consumption). Therefore, at lower CPU utilizations, the percentage of ITE power increase due to fan speed rise is anticipated to be higher than values presented in Table 2.

Finally, the test is repeated with no sealing gaskets. The results show similar elevated IPMI IAT and fan speed. However, lower pressure inside HAC and higher discrete IATs are observed which are due to the weak segregation between hot and cold aisles (the results are not presented here for the sake of space). In addition, it is perceived that the space between stacked servers in a rack is big enough to allow hot air leakage into the chassis through top perforations, i.e., stacking servers in a rack does not prevent this leakage.

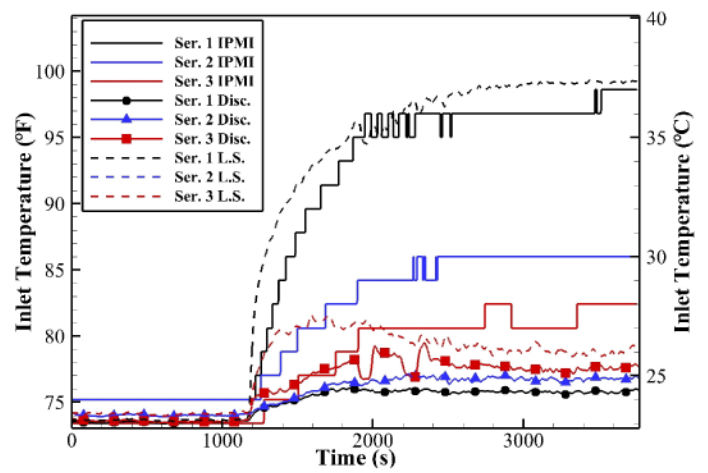


Fig. 24: IAT data for the selected servers - Scenario 2

Table 2: Maximum IPMI IAT, fan speed and ITE power increase after enclosing the hot aisle

#	S	cenario	cenario 1 Scenario 2			2
Server	Max. IPMI IAT	Fan speed (rpm)	Power increase	Max. IPMI IAT	Fan speed (rpm)	Power increase
1	97°F (36°C)	14000	19%	99°F (37°C)	14000	19%
2	97°F (36°C)	17000	22%	86°F (30°C)	6050	4%
3	95°F (35°C)	5600	2%	82°F (28°C)	5100	1%

## **CONCLUDING REMARKS**

This study investigates the importance of internal design of ITE in energy efficiency and reliability of data centers as well as the interaction between ITE and containment systems. In this paper, three commercial 2-RU servers from various generations and performance levels are tested and analyzed in various environmental conditions. Particular emphasis is placed on the cause of discrepancy between IPMI IAT and discrete sensors. Internal recirculation, hot air leakage into the server's chassis and location of IPMI IAT sensor are identified as the main causes of this discrepancy. It is observed that internal recirculation can lead to inessential elevated fan speed by affecting the IPMI IAT sensor. In addition, it is found that the extent of an internal recirculation depends on the magnitude of backpressure and can expand to the cold aisle when backpressure is strong enough. Furthermore, presence of perforations on the chassis (upstream of server fans) is found to adversely impact the performance of the servers if they are not treated properly. These perforations can allow hot air leakage from the hot zone into the server. This leakage can decrease the capacity of a server's cooling system by increasing the coolant temperature as well as decreasing fresh air pick-up from the cold aisle. In addition, this leakage can create hot spots inside ITE. Particularly, in servers 2 and 3, the IPMI IAT sensor is located in the path of the hot air leakage from the hot zone through the top perforations and consequently, IPMI IAT is affected which can lead to an elevated fan speed. It is found that presence of backpressure can enhance this leakage. An elevated fan speed naturally translates to higher power and operating costs. Besides increasing the total power consumption in a data center, an elevated fan speed can increase noise level and shorten expected fan lifetime which lowers overall reliability in data centers. In addition, elevated fan speed can increase heat dissipation from ITE which can decrease ride-through time during critical situations such as cooling failures. Also, a higher fan speed increases power draw from uninterruptable power supplies (UPS) which can limit the available uptime during power outages. Furthermore, a false high IPMI IAT can compel a data center operator to decrease SAT of cooling units which in turn increases the operating costs in a data center. Also, it is shown that air pickup in server 3 from the cold aisle can be increased by 11% by a proper segregation of the spaces up- and downstream of the fans. This in turn can improve the capacity of a server's cooling system, reduce the components temperature and lower the power consumption.

In this study, significantly different fan control strategies are seen between different server models from the same manufacturer and generation. Therefore, in a heterogeneous data center, different responses to a perturbation in environmental conditions can be expected from aisles that are populated with different ITE. In addition, it is observed that a false high IPMI IAT can cause unnecessary CPU throttling in some servers and decrease the computational performance. A surge increase in fan speed of server 2 is observed due to an open-loop safety action because of a false high IPMI IAT while the temperatures of CPUs were much lower than warning thresholds. Therefore, distributing more temperature sensors at engineered locations is

suggested to achieve a more descriptive thermal map inside the ITE as an alternative to open loop controls based on IPMI IAT solely. In addition, a surge fan speed increase in a facility can lead to a sudden change in the airflow demand as well as backpressure and consequently, cause instability in the cooling systems of a data center. Hence, a continuous fan speed control can be more desirable.

The selected servers are tested in a chimney exhaust rack to investigate the impact of internal design on the performance of ITE in a HAC system and analyze the interaction between ITE with different designs as well as the interaction between ITE and facility in a data center environment. It is observed that a false high IPMI IAT can cause a cascade increase in servers' fan speed. In addition, it is shown that internal recirculation can cause a hot air leakage from the server into the cold aisle that affects the performance of adjacent servers. In this study, the power consumption of servers 1, 2 and 3 is increased by 19%, 22% and 2%, respectively due to a false high IPMI IAT when they are tested in an under-provisioned chimney rack. Finally, it is shown that installing proper gaskets can decrease the  $\Delta T_s$  by eliminating recirculation from the hot zone through perforations on the chassis and consequently, lower the fan speed and power consumption of the servers.

#### **ACKNOWLEDGMENTS**

The authors would like to thank U. L. N. Puvvadi and A. Desu from Binghamton University Computer Science and Data Center Group. We would also like to thank the ES2 partner universities for their support and advice. This work is supported by NSF IUCRC Award No. IIP-1738793 and MRI Award No. CNS1040666.

#### **REFERENCES**

- Shehabi, A., Smith, S., Sartor, D., Brown, R., Herrlin, M., Koomey, J., Masanet, E., and Lintner, W., 2016, *United States Data Center Energy Usage Report*.
- [2] Zhou, R., Wang, Z., Bash, C. E., and McReynolds, A., 2011, "Modeling and Control for Cooling Management of Data Centers with Hot Aisle Containment," ASME 2011 Int. Mech. Eng. Congr. Expo., pp. 739–746.
- [3] Ponemon Institute LLC, 2016, 2016 Cost of Data Center Outages.
- [4] Tradat, M., Khalili, S., Sammakia, B. G., Ibrahim, M., Peddle, T., Calder, A. R., Dawson, B., Seymour, M., Nemati, K., and Alissa, H., 2017, "Comparison and Evaluation of Different Monitoring Methods in a Data Center Environment," ASME 2017 International Technical Conference and Exhibition on Packaging and Integration of Electronic and Photonic Microsystems, InterPACK 2017, Collocated with the ASME 2017 Conference on Information Storage and Processing Systems.
- [5] Sundaralingam, V., Arghode, V. K., Joshi, Y., and Phelps, W., 2014, "Experimental Characterization of Various Cold Aisle Containment Configurations for Data Centers," J. Electron. Packag., 137(1), p. 11007.

- [6] Makwana, Y. U., Calder, A. R., and Shrivastava, S. K., 2014, "Benefits of Properly Sealing a Cold Aisle Containment System," Thermomechanical Phenom. Electron. Syst. -Proceedings Intersoc. Conf. ITherm2014, pp. 793–797.
- [7] Khalili, S., Tradat, M., Nemati, K., Seymour, M., and Sammakia, B., 2018, "Impact of Tile Design on the Thermal Performance of Open and Enclosed Aisles," J. Electron. Packag., 140(1), pp. 10907-10907-12.
- [8] Nemati, K., Alissa, H. A., Murray, B. T., and Sammakia, B., 2016, "Steady-State and Transient Comparison of Cold and Hot Aisle Containment and Chimney," In Thermal and Thermomechanical Phenomena in Electronic Systems (ITherm), 15th IEEE Intersociety Conference on, pp. 1435–1443.
- [9] Khalili, S., Alissa, H., Desu, A., Sammakia, B., and Ghose, K., 2018, "An Experimental Analysis of Hot Aisle Containment Systems," The Intersociety Conference on Thermal and Thermomechanical Phenomena in Electronic Systems (ITherm 2018), San Diego, CA USA, p. Accepted Paper.
- [10] Niemann, J., Brown, K., and Avelar, V., 2011, "Impact of Hot and Cold Aisle Containment on Data Center Temperature and Efficiency," Schneider Electr. Data Cent. Sci. Center, White Pap., 135, pp. 1–14.
- [11] Alissa, H. A., Nemati, K., Sammakia, B. G., Seymour, M. J., Tipton, R., Mendo, D., Demetriou, D. W., Schneebeli, K., Tipton, R., Mendo, D., Demetriou, D. W., and Schneebeli, K., 2016, "Chip to Chiller Experimental Cooling Failure Analysis of Data Centers: The Interaction Between IT and Facility," IEEE Trans. Components, Packag. Manuf. Technol., 6(9), pp. 1361–1378.
- [12] Tradat, M. I., Alissa, H. A., Nemati, K., Khalili, S., Sammakia, B. G., Seymour, M. J., and Tipton, R., 2017, "Impact of Elevated Temperature on Data Center Operation Based on Internal and External IT Instrumentation," Annu. IEEE Semicond. Therm. Meas. Manag. Symp.
- [13] TMP75 Datasheet, "Texas Instruments" [Online]. Available: http://www.ti.com/lit/ds/symlink/tmp75.pdf.
- [14] Great Internet Mersenne Prime Search, 2015, "Mprime (Prime95)" [Online]. Available: https://www.mersenne.org/download/.
- [15] Alissa, H. A., Nemati, K., Sammakia, B., Seymour, M., Schneebeli, K., and Schmidt, R., 2015, "Experimental and Numerical Characterization of a Raised Floor Data Center Using Rapid Operational Flow Curves Model," ASME 2015 International Technical Conference and Exhibition on Packaging and Integration of Electronic and Photonic Microsystems Collocated with the ASME 2015 13th International Conference on Nanochannels, Microchannels, and Minichannels, American Society of Mechanical Engineers, p. V001T09A016.